Highly Refractive and Transparent Polyimides Derived from 4,4′-[*m*-Sulfonylbis(phenylenesulfanyl)]diphthalic Anhydride and Various Sulfur-Containing Aromatic Diamines

Jin-gang Liu, Yasuhiro Nakamura, Yasuo Suzuki, Yuji Shibasaki, Shinji Ando, and Mitsuru Ueda*

Department of Organic and Polymeric Materials, Tokyo Institute of Technology, 2-12-1-H120, O-okayama, Meguro-ku, Tokyo 152-8552, Japan

Received June 20, 2007; Revised Manuscript Received August 15, 2007

ABSTRACT: We have developed highly refractive and transparent polyimides (PIs). The PIs were prepared from a newly developed *meta*-substituted sulfonyl-bridged dianhydride, 4,4′-[*m*-sulfonylbis(phenylenesulfanyl)]-diphthalic anhydride (DPSDA), and various sulfur-containing aromatic diamines, including 4,4′-thiobis[(*p*-phenylenesulfanyl)aniline] (3SDA), 4,4′-sulfonylbis[(*p*-phenylenesulfanyl)aniline] (BADPS), 2,8-bis(*p*-aminophenylenesulfanyl)dibenzothiophene (APDBT), and 2,7-bis(*p*-aminophenylenesulfanyl)thianthrene (APTT), by employing a two-step polycondensation procedure. The PIs exhibited good thermal stabilities such as the relatively high glass-transition temperatures in the range of 177−206 °C and high initial thermal decomposition temperatures ($T_{5\%}$) exceeding 470 °C. The *meta*-substituted electron-withdrawing sulfonyl moiety endowed the PI films with good optical transparency. The optical transmittances of the PI films at 450 nm were higher than 85% for the thickness of approximately 10 μm. Furthermore, the flexible thioether linkages and sulfonyl moiety in the molecular chains of the PIs provided them with high refractive indices of 1.7162−1.7432, relatively small Abbe numbers of 14.1−14.8, and low birefringences of 0.0059−0.0065.

Introduction

The achievement of new functions of advanced optical devices is becoming increasingly dependent on the availability of new functional materials.[1−3] Recently, high refractive index (high-*n*) polymers have attracted much attention for their potential applications in advanced optoelectronic fabrications such as high performance substrates for advanced display devices,[4,5] optical adhesives or encapsulants for organic light-emitting diode devices (OLED),[6,7] antireflective coatings for advanced optical applications,[8] and microlens components for charge-coupled devices (CCD) or complementary metal oxide semiconductor (CMOS) image sensors (CIS).[9] The typical refractive indices of conventional polymers are often in the range of 1.3−1.7.[10] However, with regard to practical applications, for instance, microlens materials for CIS, a refractive index exceeding 1.7 is frequently desired. According to the Lorentz−Lorenz equation, the introduction of substituents with high molar refractions and low molar volumes can efficiently increase the refractive indices of polymers.[11] It has been well-established that aromatic ring,[12] halogen atoms except fluorine,[13] sulfur atoms[14,15] and metal atoms[16] are effective in increasing the refractive indices. Another effective approach to increase the refractive indices of organic polymers is to combine the polymer matrix with high-*n* inorganic nanoparticles, i.e., to develop organic−inorganic nanocomposites.[17−19] Although high-*n* polymers can be developed by the aforementioned procedures, several other requirements have to be addressed for the practical applications such as low birefringence (Δn), good transparency in the visible light region, and high thermal stability. In addition, the good pattern formability afforded by the conventional photolithography technique is often required in view of the processing procedure of optical devices.[20] Taking all of the abovementioned requirements into consideration, sulfur-containing high-*n* polymers might be one of the most promising candidates for high-tech optical applications.

In our continuous efforts to develop practical high-*n* polymers, sulfur-containing polyimides (PIs) attracted our attention. PIs are well-known for their excellent combined properties, especially their high thermal stability and inherent high refractive index.[21−23] Several PIs containing thioether linkages, either linear[24−25] or cyclic,[26,27] have been prepared in our laboratory. As reported recently, refractive indices as high as 1.76 at the wavelength of 632.8 nm and birefringences lower than 0.01 have been successfully achieved.[27] However, when fabricating optical devices, optical transparency might be one of the most serious obstacles for high-*n* PIs. The formation of intermolecular or intramolecular charge-transfer complexes (CTCs) between the electron-donating diamine moiety and the electron-accepting dianhydride moiety often result in the deep coloration of the PI films in the visible light regions.[28,29] Numerous efforts have been made to decrease the coloration of conventional PIs. However, most of these procedures, such as the introduction of electron-withdrawing fluoro-containing substituents or alicyclic moiety, often simultaneously decrease the refractive indices of the PIs.[30] Thus, the development of high-*n* PIs with high optical transparency is a challenging topic.

In this study, a *meta*-substituted dianhydride containing both sulfonyl and thioether moieties, 4,4′-[*m*-sulfonylbis(phenylenesulfanyl)]diphthalic anhydride (DPSDA), was designed and synthesized. The *meta*-substituted structure and the bulky electronegative sulfonyl moiety are expected to endow the PIs with high transparency due to the weakened CTC formation and expanded free volumes. The flexible thioether linkage would be beneficial to maintain the high refractive indices and low birefringences of the PI films. The effects of the structure on the thermal and optical properties of the PIs were investigated in detail.

* To whom correspondence should be addressed. E-mail: ueda.m.ad@m.titech.ac.jp. Telephone: +81-3-57342127. Fax: +81-3-57342127.

10.1021/ma0713714 CCC: $37.00
Published on Web 10/02/2007

Experimental Section

Materials. All the chemicals were purchased from TCI (Tokyo, Japan) except described specially. Diphenylsulfone and 4-bromophthalic anhydride were used as received. *N*-Methyl-2-pyrrolidinone (NMP, Wako, Japan) and *N, N*-dimethylformamide (DMF, Wako, Japan) were purified by vacuum distillation over CaH_2 prior to use. 4,4′-Thiobis[(*p*-phenylenesulfanyl)aniline] (3SDA),[25] 2,8-bis(*p*-aminophenylenesulfanyl)dibenzothiophene (APDBT),[26] and 2,7-bis(*p*-aminophenylenesulfanyl)thianthrene (APTT)[27] were synthesized in our laboratory according to our previous work. 4,4′-Sulfonylbis-[(*p*-phenylenesulfanyl)aniline] (BADPS) was synthesized according to the literature.[31]

Monomer Synthesis. *Diphenylsulfone-3,3′-disulfonyl chloride (I).* A 250 mL three-necked flask was equipped with a magnetic stirrer and a reflux condenser. The flask was charged with diphenylsulfone (23.8 g, 0.11 mol) and chlorosulfonic acid (58 mL, 0.87 mol). The reaction mixture was heated to 140 °C and maintained at this temperature for 4 h. Then the mixture was cooled to room temperature and carefully poured into ice−water (500 mL). The precipitated white solid was filtered, washed thoroughly with water, and dried in vacuo at 80 °C for 24 h. The obtained white solid was recrystallized from acetic acid to afford white crystals. Yield: 32.9 g (72.0%); mp: 181.0 °C (by DSC). FT-IR (KBr, cm^{-1}): 1581.3, 1423.2, 1376.9, 1342.2, 1307.5, 1187.9, 1157.1, 1076.1, 813.8, and 567.0. ^{1}H NMR (300 MHz, $CDCl_3$, ppm): 7.85−7.91 (t, 2H), 8.28−8.36 (m, 4H), and 8.61−8.62 (m, 2H). Elem. Anal. Calcd for $C_{12}H_8Cl_2O_6S_3$: C, 34.71%; H, 1.94%. Found: C, 34.88%; H, 2.15%.

Diphenylsulfone-3,3′-dithiol (II). A 250 mL three-necked flask equipped with a magnetic stirrer and a reflux condenser was charged with stannous chloride dihydrate (50 g, 0.22 mol), acetic acid (100 mL), and hydrochloric acid (40 mL). The reaction mixture was heated to 90 °C, and I (4.15 g, 0.01 mol) was added with stirring. The mixture was maintained at 90 °C for 3 h and then cooled to room temperature. The reaction mixture was carefully poured into water (200 mL) containing hydrochloric acid (20 mL). The obtained solid was filtered, washed thoroughly with water, and dried in vacuo at 80 °C for 24 h. The obtained pale-yellow solid was used in the next step without further purification. Yield: 2.57 g (91.0%); mp: 107.5 °C (by DSC). FT-IR (KBr, cm^{-1}): 2553.3, 1581.3, 1461.8, 1415.5, 1319.1, 1295.9, 1160.9, 1130.1, 1072.2, 775.2, 678.8, and 601.7. ^{1}H NMR (300 MHz, $CDCl_3$, ppm): 3.64 (s, 2H), 7.34−7.46 (m, 4H), 7.67−7.70 (d, 2H), and 7.81−7.82 (m, 2H). Elem. Anal. Calcd for $C_{12}H_{10}O_2S_3$: C, 51.04%; H, 3.57%. Found: C, 50.79%; H, 3.61%.

4,4′-[m-Sulfonylbis(phenylenesulfanyl)]diphthalic anhydride (DPSDA). A three-necked 250 mL flask equipped with a magnetic stirrer, a nitrogen inlet, and a condenser was charged with a mixture of II (2.82 g, 0.01 mol), 4-bromophthalic anhydride (5.00 g, 0.022 mol), anhydrous K_2CO_3 (3.04 g, 0.022 mol), and freshly distilled *N,N*-dimethylformamide (50 mL). The mixture was heated to 120 °C in nitrogen for 12 h. Then the mixture was cooled to room temperature, and the white solid was collected by filtration and dried in vacuo at 160 °C for 24 h. The obtained white powder was boiled with concentrated hydrochloric acid (50 mL) for 3 h. After the mixture was cooled to room temperature, the white solid (tetra-acid III) was collected by filtration and washed thoroughly with cold water. The obtained solid was first heated in vacuo (∼0.01 mmHg) at 120 °C to remove the water, then it was heated in vacuo at 160−180 °C for 3 h to afford the dianhydride DPSDA as pale-yellow crystals. Yield: 4.20 g (73.1%); mp: 193.3 °C (DSC peak temperature). FT IR (KBr, cm^{-1}): 1851.3, 1774.2, 1604.5, 1461.8, 1423.2, 1326.8, 1295.9, 1257.4, 1160.9, 902.5, 732.8, 686.5, and 605.5. ^{1}H NMR (300 MHz, $CDCl_3$, ppm): 7.57−7.59 (d, 2H), 7.62−7.67 (m, 4H), 7.73−7.78 (d, 2H), 7.86−7.90 (d, 2 h), and 8.10−8.12 (m, 2H). ^{13}C NMR (300 MHz, DMSO-d_6, ppm): 163.4, 147.2, 143.1, 139.5, 135.7, 134.2, 133.5, 132.8, 132.5, 129.9, 129.4, 127.1, and 124.6. Elem. Anal. Calcd for $C_{28}H_{14}O_8S_3$: C, 58.53%; H, 2.46%. Found: C, 58.19%; H, 2.73%.

Polyimide Synthesis. The general polycondensation procedure can be illustrated by the synthesis of PI-1 as follows. To a 200 mL three-necked flask equipped with a mechanical stirrer, a nitrogen inlet, and a cold water bath was added 3SDA (4.3262 g, 10.0 mmol) and freshly distilled NMP (30.0 g). A clear diamine solution was obtained after stirring for 30 min. Then, DPSDA (5.7459 g, 10.0 mmol) was added in three portions to the stirred solution, followed by washing with additional NMP (10.3 g), and the solid content of reaction mixture was adjusted to 20% by weight at the same time. The reaction mixture was stirred in nitrogen at room temperature for 24 h to afford a viscous pale-brown solution. The obtained poly(amic acid) (PAA) solution was diluted by adding additional NMP (50.0 g) to adjust the solid content to be 10% by weight. The PAA solution was filtered through a 0.45 μm Teflon syringe filter to eliminate any particulates that might affect the quality of the cured film. ^{1}H NMR (300 MHz, DMSO-d_6, ppm): 7.14−7.26 (m, 8H), 7.40−7.42 (m, 8H), 7.58−7.78 (m, 10H), 7.84−7.90 (m, 4H), and 10.47−10.50 (m, 2H).

The purified PAA solution was spin-coated on a silicon (Si) wafer or quartz substrate, and the thickness was controlled by regulating the spinning rate. The thickness of the specimen for Fourier transform infrared (FT-IR) and ultraviolet−visible (UV−vis) measurements was controlled to be approximately 10 μm, and the thickness of the specimen to be used for measuring thermal properties was adjusted to be 30−50 μm. The PI-1 film was obtained by thermally curing the PAA solution in an oven at 80, 150, 250, and 300 °C for 1 h each under nitrogen. The PI-1 film, which was pale-yellow in color at the thickness of 10 μm, was obtained by immersing the Si wafer in warm water.

The other PI films were prepared by a similar procedure mentioned above, except that 3SDA was replaced by BADPS (PI-2), APDBT (PI-3), or APTT (PI-4), respectively.

Measurements. The ^{1}H and ^{13}C NMR spectra were recorded on a Varian Mercury 300 spectrometer using $CDCl_3$ or DMSO-d_6 as solvent and tetramethylsilane as reference. The ^{13}C DEPT-135 (distortionless enhancement by polarization transfer) experiment was done by using DMSO-d_6 as the solvent. Inherent viscosity was measured using an Ubbelohde viscometer with a 0.5 g/dL NMP solution at 30 °C. The Fourier transform infrared (FT-IR) spectra were obtained with a Horiba FT-120 Fourier transform spectrophotometer. The ultraviolet−visible (UV−vis) spectra were recorded on a Hitachi U-3210 spectrophotometer at room temperature. PI films were dried at 100 °C for 1 h before testing to remove the absorbed moisture. The wide-angle *X*-ray diffraction (XRD) was conducted on a Rigaku D/max-2500 X-ray diffractometer with Cu Kα1 radiation, operated at 40 kV and 200 mA. Thermogravimetric analysis (TGA) was recorded on a Seiko TG/DTA 6300 thermal analysis system at a heating rate of 10 °C/min in nitrogen. Differential scanning calorimetry (DSC) was performed on a Seiko DSC 6300 at a heating rate of 10 °C/min. Dynamic mechanical thermal analysis (DMA) was performed on PI film specimens (30 mm long, 10 mm wide, and 50−60 μm thick) on a Seiko DMS 6300 at a heating rate of 2 °C/min with a load frequency of 1 Hz in air. The glass transition temperature (T_g) was determined as the peak temperature of the loss modulus (E'') plot.

The out-of-plane (n_{TM}) and in-plane (n_{TE}) refractive indices of PI films were measured with a prism coupler (Metricon, model PC-2000) equipped with a He−Ne laser light source (wavelength: 632.8 nm). The polarization of the incident light guided from a linearly polarized He−Ne laser was controlled by inserting a half waveplate in the light path. The prism attachable to the surface of PI films was made of a single crystal of gallium gadolinium garnet (GGG).

In-plane (n_{TE})/out-of-plane (n_{TM}) birefringence (Δn) was calculated as a difference between n_{TE} and n_{TM}. The average refractive index (n_{av}) was calculated according to eq 1:

$$n_{AV} = \sqrt{(2n_{TE}^2 + n_{TM}^2)/3} \quad (1)$$

In addition, the wavelength dispersion of refractive indices in the visible region were measured with a multiwavelengths Abbe refractometer (Atago, model DR-M2) equipped with a halogen

Scheme 1. Synthesis of DPSDA

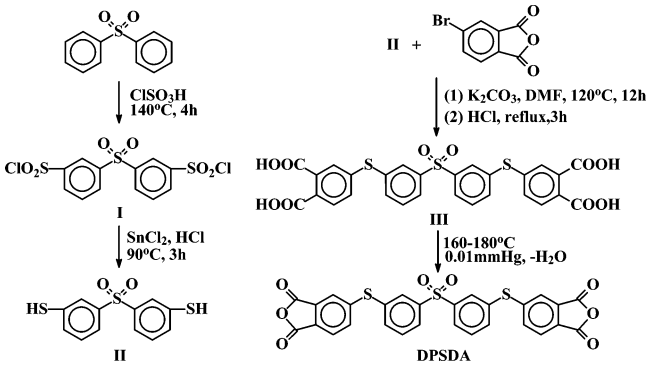

Scheme 2. Synthesis of PIs

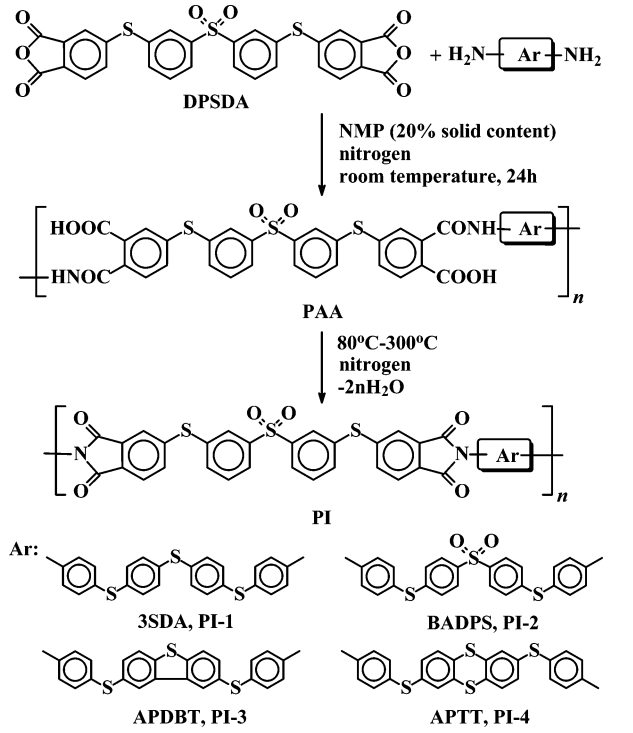

illuminating lamp and interference filters at the wavelengths of 486, 589, and 656 nm. The n_{TE} and n_{TM} of PI films were selectively measured by inserting a linear polarizing film in the light path. The values of n_{av} were calculated according to eq 1, and the Abbe number (ν_D), which represents the degree of wavelength dispersion, was calculated according to eq 2:

$$\nu_D = \frac{n_{589} - 1}{n_{486} - n_{656}} \tag{2}$$

where n_{486}, n_{589}, and n_{656} are the average refractive indices measured at 486, 589, and 656 nm, respectively.

On the other hand, the average refractive indices measured at the three wavelengths (n_λ) can be fitted using the simplified Cauchy formula,

$$n_\lambda = n_\infty + \frac{D}{\lambda^2} \tag{3}$$

where λ is the wavelength, n_∞ is the estimated refractive index at infinite wavelength, and D is the coefficient of dispersion. A larger D indicates significant wavelength dispersion, and a high n_∞ corresponds to an inherent high refractive index without the influence of absorptions located at shorter wavelengths.

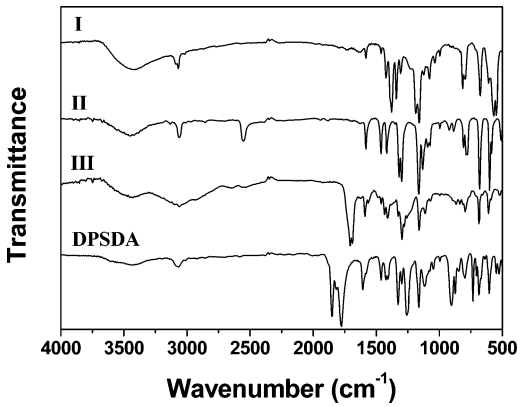

Figure 1. FT IR spectra of DPSDA and the intermediates (KBr).

Calculation. The refractive indices of the aromatic PIs synthesized in this study were calculated on the base of Lorentz−Lorenz theory as reported previously.[24] One-electron transition energies and the corresponding oscillator strengths of the PIs were also calculated using the time-dependent density functional theory (TD-DFT) to predict the optical absorption in the UV−visible region.[32] The 6-311G(d) basis set was used for geometry optimizations under no constraints, and the 6-311++G(d,p) was used for calculations of linear polarizabilities, transition energies, and oscillator strengths. The three-parameter Becke-style hybrid functional (B3LYP) was adopted as a function, and all the calculations were performed using the software package of Gaussian-03 (revisions C02 and D01). A typical packing coefficient (K_p) of 0.60 was used for evaluating the intrinsic molecular volumes of models to predict the refractive indices.[22]

Results and Discussion

Monomer Synthesis. The *meta*-substituted sulfonyl-bridged dianhydride, DPSDA, was synthesized directly from 4-bromophthalic anhydride and diphenylsulfone-3,3′-dithiol (II) in the presence of anhydrous potassium carbonate in DMF at 120 °C for 12 h; this was followed by dehydration at elevated temperatures in high vacuo with a yield exceeding 75% (Scheme 1). This procedure has been well established in the literature for bis(ether anhydride) or bis(thioether anhydride) synthesis.[25,33] The dianhydride was obtained as pale-yellow crystals. The characterization result showed that the purity of the dianhydride was sufficiently high for the subsequent polymerization. The dianhydride could be further purified by recrystallization from an acetic anhydride/petroleum ether mixture (1:2, v/v). Figure 1 presents the FT-IR spectra of the dianhydride and intermediates. The characteristic absorption of carbonyl in carboxylic acid (III) located at 1708 cm^{-1} disappears in the spectrum of DPSDA. Instead, the typical absorptions of anhydride carbonyl at 1851 and 1774 cm^{-1} are distinctly observed. The characteristic absorptions due to sulfonyl (SO_2) groups at 1320 and 1160 cm^{-1} are observed in both of the dianhydride and intermediates. In addition, the typical absorptions of thioether (Ar−S−Ar) linkages appear at 1257 cm^{-1} in the dianhydride spectrum. The ^1H and ^{13}C NMR spectra are shown in parts a and b of Figure 2, respectively, together with the assignment of the observed resonance. No extra peaks are observed. The protons ortho to the anhydride moiety (H_a and H_b) appeared at the lowest field in the spectrum, and the proton ortho to the electron-withdrawing sulfone group (H_g) is observed at 7.73−7.78. In the ^{13}C NMR spectrum, 12 signals are clearly revealed due to the structure symmetry; among these, seven carbons induce signals in the DEPT-135 measurements due to the existence of the attached protons. In addition, elemental analysis results also supported the formation of the dianhydride.

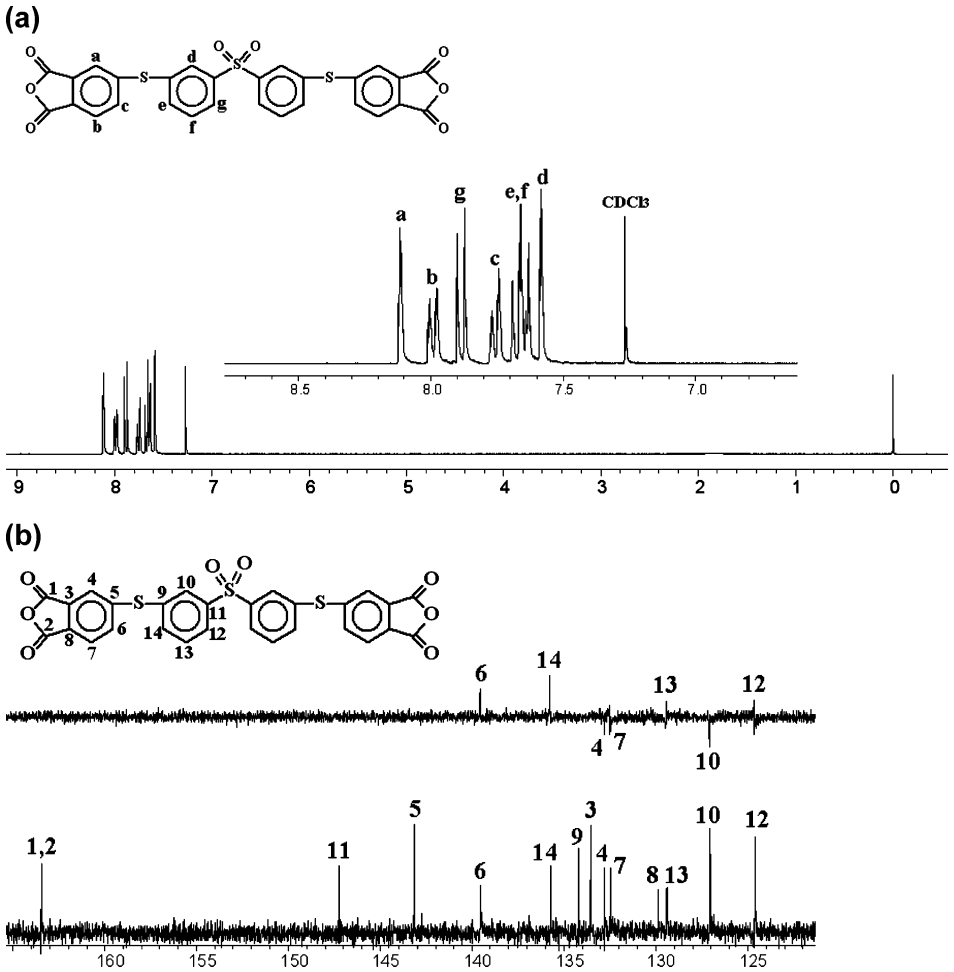

Figure 2. ^{1}H NMR and ^{13}C NMR spectra of DPSDA (300 MHz). (a) DPSDA, ^{1}H NMR, $CDCl_3$; (b) DPSDA, ^{13}C DEPT-135 (upper) and ^{13}C NMR (lower), DMSO-d_6).

Polyimide Synthesis. A series of PIs were synthesized by employing a two-step polycondensation procedure of DPSDA with four sulfur-containing diamines via the soluble poly(amic acid) (PAA) precursors, followed by thermal imidization at elevated temperatures (Scheme 2). The diamines employed for the polymerization have their own special characteristics. For example, 3SDA containing flexible linear thioether linkages is expected to afford PIs with high n_{av}, low Δn, good transparency, and low T_g at the same time. APDBT and APTT containing cyclic thioether moieties possess higher sulfur contents. Thus, the PIs derived from these two diamines are expected to have higher n_{av} and higher T_g values. On the other hand, the optical transparency might be sacrificed to some extent due to the enhanced π-conjugation in the molecule chains and the resultant CTC formation. BADPS contains both thioether and sulfonyl linkages; thus, in this case, the optical transparency should be improved owing to the reductions in both the chain−chain electronic interaction in the PIs caused by the incorporation of bulky sulfonyl moiety and the conjugation by the *meta*-substituted structures.[34] However, the n_{av} values might be decreased due to the bulky molecular volume of the sulfonyl group. Thus, it is interesting to examine the effects of the diamine structures on the properties of the obtained PIs, which could aid us in further determining the compromise to be made among the desired properties.

The inherent viscosities of the PAAs are in the range of 0.62−0.81 dL g^{-1}, indicating the high reactivity and high purity of the starting monomers. Flexible and tough PI films were obtained by casting the PAA precursors, which confirmed the high molecular weights of the PAAs.

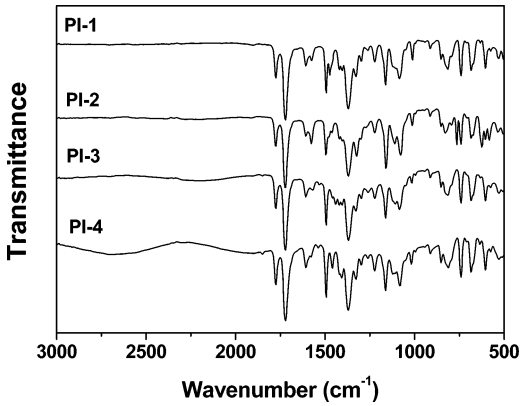

Figure 3. FT IR spectra of PI films.

The successful thermal conversion from PAAs to PIs can be confirmed by the FT-IR spectra shown in Figure 3; in this figure, the characteristic absorptions due to the imide moiety at ∼1780 cm^{-1} ($\upsilon_{as,C=O}$), ∼1720 cm^{-1} ($\upsilon_{s,C=O}$), and 1380 cm^{-1} (υ_{C-N}) can be clearly identified. In addition, the typical absorption of the sulfonyl groups located at 1320 and 1160 cm^{-1} can also be observed.

The wide-angle X-ray diffraction spectra depicted in Figure 4 indicate that the present PIs demonstrate typical amorphous natures, which can mainly be attributed to the inhibition of crystallization due to the flexible thioether linkage and the bulky sulfonyl moiety in the PI chains.

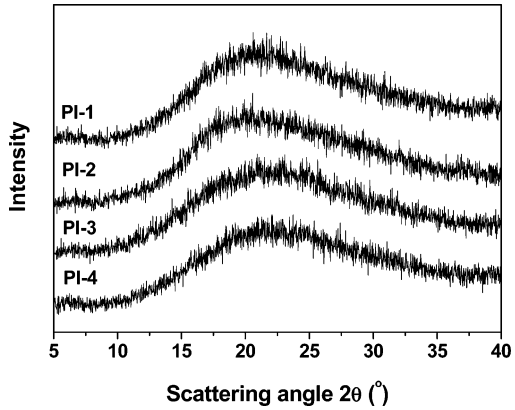

Figure 4. Wide-angle X-ray diffraction patterns.

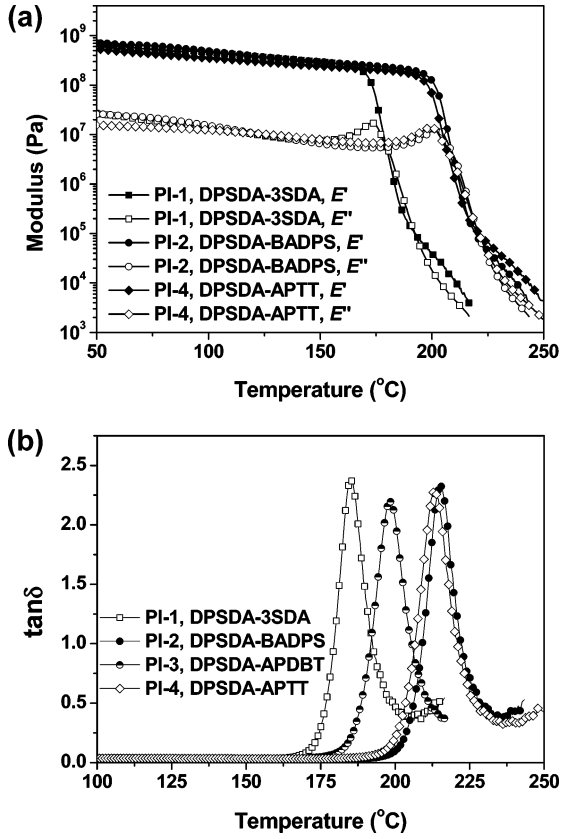

Figure 5. DMA curves of PIs (1 Hz, 2 °C/min, in air). (a) Storage modulus E' and loss modulus E''; (b) tan δ.

Thermal Properties. The thermal decomposition and deformation behaviors of the PIs were investigated by TGA, DSC, and DMA measurements. The results are presented in Table 1. According to the TGA results, the PIs maintained nearly 100% of their original weights up to 400 °C and more than 50% of their weights at 750 °C in nitrogen. PI-2 exhibited the lowest thermal stability with the 5% and 10% weight loss temperatures of 474 and 494 °C, respectively. In fact, sulfonyl-containing PIs have been characterized by their inferior thermal stability as compared to their common rigid analogs.[35]

The glass-transition temperatures (T_gs) of the PIs were determined by DSC and DMA measurements. T_g is one of the key parameters for high-*n* optical polymers when considering the high-temperature circumstance during fabrication and the long-term heat-releasing environment resulting from the miniaturization of the optoelectronic devices.[36] All of the PI films exhibited T_g values exceeding 200 °C except PI-1. PI-2 has a T_g of 207 °C, which is nearly 30 °C higher than that of PI-1;

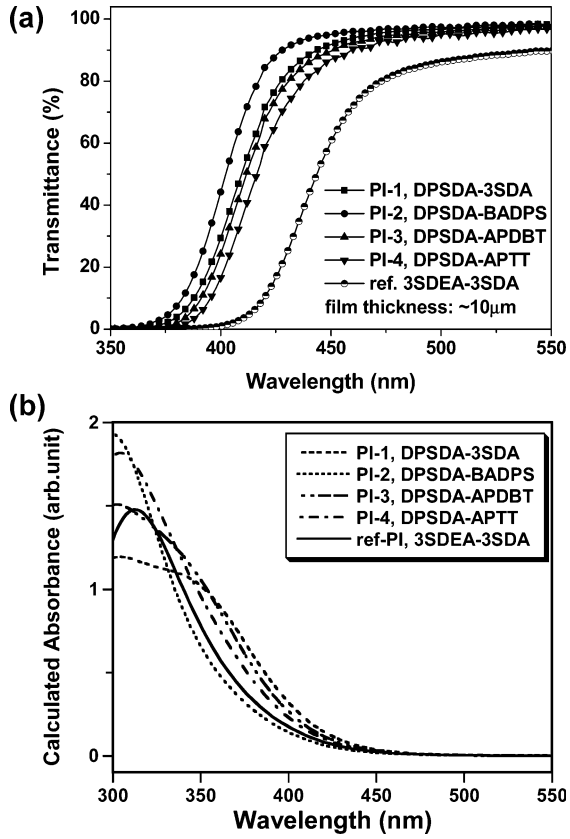

Figure 6. Experimental (top) and calculated (bottom) UV−vis spectra of the PI films.

Table 1. Polymerization and Thermal Properties of PIs

PI	$[\eta]_{inh}$[a] (dL/g)	film[b]	T_g (°C)[c] DSC	T_g (°C)[c] DMA	$T_{5\%}$[c] (°C)	$T_{10\%}$[c] (°C)	R_{w750}[c] (%)
PI-1	0.78	pale-yellow	178	174	490	511	55
PI-2	0.62	pale-yellow	207	203	474	494	52
PI-3	0.74	pale-brown	203	195	476	506	60
PI-4	0.81	pale-brown	205	199	475	498	64

[a] Measured with PAA at a concentration of 0.5 g/dL in NMP at 30 °C. [b] Color at the thickness of approximately 10 μm. [c] T_g: glass transition temperature; $T_{5\%}$, $T_{10\%}$: temperatures at 5% and 10% weight loss, respectively; R_{w750}: residual weight ratio at 750 °C in nitrogen.

this could mainly be attributed to the higher intermolecular interactions and the steric hindrance of the bulky sulfonyl moiety. Apparently, the T_g values of the proposed PIs are slightly lower than those of commercial ether-containing high-temperature polymers such as polyetherimides Ultem1000 (T_g: 218 °C),[37] and poly(aryl ether sulfone) (PES, T_g: 223 °C).[38]

Figure 5 illustrates the variations in the storage modulus (E'), loss modulus (E''), and loss factor (tan δ) with the temperatures as detected by DMA measurements. It can be seen from Figure 5a that the modulus retains constant or decreased slightly before the corresponding T_gs. After T_gs, which is determined as the peak temperature of E'', the modulus drops dramatically. PI-1, derived from DPSDA and linear 3SDA, and PI-2, derived from BADPS, exhibit the lowest T_g (174 °C) and the highest (203 °C) T_g, respectively. The T_gs of PIs containing cyclic thioether linkages (PI-3 and PI-4) are similar to that of PI-2. This trend is in good agreement with the results obtained from the DSC measurements. These results reveal that the heat deflection temperatures of the PIs can be improved by the incorporation of bulky or cyclic substituents.

Table 2. Optical Properties of PI Films

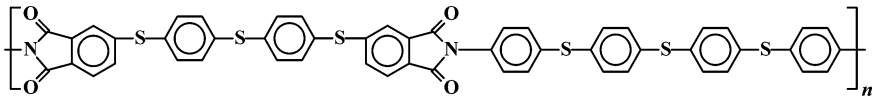

PI	S_C[a] (wt%)	λ_{cutoff}[b] (nm)	T_{450}[c] *(%)*	d[d] (μm)	refractive indices and birefringence				
					n_{TE}[e]	n_{TM}[e]	n_{av}[e]	Δn[e]	n_{cal}[f]
PI-1	19.81	374	92	5.4	1.7329	1.7269	1.7309	0.0059	1.7400
PI-2	19.18	365	95	3.6	1.7182	1.7121	1.7162	0.0061	1.7095
PI-3	19.85	380	89	3.1	1.7426	1.7367	1.7406	0.0059	1.7480
PI-4	22.41	385	87	4.5	1.7453	1.7388	1.7432	0.0065	1.7537
ref-PI[g]	20.48	402	60	9.3	1.7505	1.7437	1.7482	0.0068	1.7708

[a] Sulfur content. [b] Cutoff wavelength. [c] Transmittance at 450 nm. [d] Film thickness. [e] Measured at 632.8 nm, see Measurements section. [f] Calculated refractive index, see Calculation section. [g] 3SDEA-3SDA with the chemical structure as given above.[25]

Optical Properties. *Meta*-substituted sulfonyl-bridged PIs have been proposed as colorless or pale-colored coatings for advanced high-tech applications.[39,40] The importance of the electron-withdrawing characteristics of sulfonyl moiety has been well noticed. However, thus far, the contribution of sulfonyl group to the refractive index of the polymers has rarely been addressed. The UV−vis spectra of the PI films with thicknesses of approximately 10 μm are shown in Figure 6 (top), and the optical data are summarized in Table 2. The cutoff wavelengths (λ_{cutoff}), which are determined by the wavelengths corresponding to the intersection points of the line tangent to the UV−vis curves, are in the range of 365−385 nm. The transmittances of the films measured at 450 nm are entirely higher than 85%, which is much higher than that of the reference PI (ref-PI) derived from 4,4′-[*p*-thiobis(phenylenesulfanyl)]diphthalic anhydride (3SDEA) and 3SDA.[25] In particular, PI-2 containing bridging sulfonyl groups both in the dianhydride and diamine moieties exhibits the highest optical transparency, which is attributable to the reduction of the intermolecular interactions by the bulky sulfonyl substituents and the inhibition of CTC formation due to the reduction of the electron-donating ability of the diamine originating from the electron-withdrawing sulfonyl group. The calculated absorption spectra are also shown in Figure 6 (bottom). Note that the values of λ_{cutoff} of all the PIs are similar; this indicates that the experimentally observed relatively lower transparency of the ref-PI can be attributed to the enhanced intermolecular interactions caused by thioether substituents. The thioether linkages are more likely to form well-packed intermolecular orderings stabilized by the CTC formation, which is in contrast to the sulfonyl group.

As listed in Table 2, the in-plane (n_{TE}) and out-of-plane (n_{TM}) refractive indices of the PI films measured at 632.8 nm range from 1.7182 to 1.7453 and 1.7121 to 1.7388, respectively. The fact that the n_{TE} values of the PI films are slightly higher than the n_{TM} ones implies that the chain orientation parallel to the film plane is more dominant than that perpendicular to the plane. The average refractive indices (n_{av}) estimated from the n_{TE} and n_{TM} values are in the range between 1.7162 and 1.7432 in the following order: PI-2 (1.7162) < PI-1 (1.7309) < PI-3 (1.7406) < PI-4 (1.7432). This trend is consistent with the refractive indices (n_{cal}) calculated by DFT, and all the n_{av} values are significantly higher than those of conventional optical polymers such as poly(methylmethacrylate) (PMMA, 1.489), polystyrene (PS, 1.585), and polycarbonate (PC, 1.577). A comparison of the n_{av} values of PI-1, PI-2, and ref-PI indicates that the substitution of one and two sulfonyl linkages (−SO_2−) for thioether linkages (−S−) in the main chain reduces the n_{av} by 0.0173 (ref-PI → PI-1) and 0.0320 (ref-PI → PI-2), respectively. These systematic decreases in n_{av} are attributable to the lower polarizability per unit volume of −SO_2− as compared to −S−. In particular, the two oxygen atoms in −SO_2− significantly increase the molecular volume of the linkage and reduce the content of polarizable sulfur atoms in the PIs. In addition, −SO_2− renders the reduction of the intermolecular CTC formation and the electron-donating ability of the diamine. A distinct tradeoff relationship exists between the refractive indices and the optical transparency, as seen from Figure 6 and Table 2. A higher −SO_2− content improves the optical transparency but also results in a lower refractive index. In contrast, the introduction of dibenzothiophene ring (PI-3) and thianthrene ring (PI-4) significantly increases the values of *Sc* and n_{av}; however, they result in a slight deterioration in the optical transparency, as mentioned above. The coefficients of molecular packing (K_p) estimated from the calculated molecular polarizabilities and experimental n_{av} values are 0.595, 0.604, 0.596, 0.594, and 0.587 for PI-1, PI-2, PI-3, PI-4, and ref-PI, respectively. It is interesting to note that the highest K_p value was obtained for PI-2, which contains two −SO_2− linkages in the main chain; this demonstrates that −SO_2− does not reduce the degree of molecular packing but decreases the polarizability per volume. The highest n_{av} observed for PI-4 (1.7432) is slightly lower than that of ref-PI (1.7482), but the better transparency of the former (pale-yellow color for a 10 μm thick film) as compared to the latter (pale-brown color for the same thickness film) should be useful for certain optical applications utilizing the entire range of visible wavelengths (e.g., 400−800 nm).

In addition, wavelength dispersion of refractive index is an important property of optical materials. Abbe number (ν_D) has been frequently used as a measure of the degree of dispersion in the visible region. In general, larger values of ν are expected because smaller dispersion of refractive index is preferable for conventional optical applications such as lens and waveplates. The refractive indices of PI films thus measured at the wavelengths of 486, 589, and 656 nm are listed in Table 3 and plotted in Figure 7. These wavelengths represent the three primary colors (blue, green, and red). Compared with the optical polymers of PMMA ($\nu_D = 57$), PS ($\nu_D = 30$), and PC ($\nu_D = 29$), the dispersion of PIs are significantly larger, as demonstrated by the ν_D values of 14.1−14.8. This is because the λ_{cutoff} of PIs (365−385 nm) are located near the boundary between the UV and visible regions, which leads to that the imaginary part k of the complex refractive index $n^* = n - ik$ reaches a significant value ($k \sim 10^{-3}$) in the visible region. The estimated

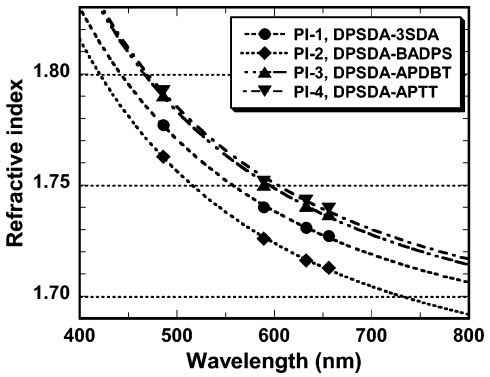

Figure 7. Wavelength dispersion of average refractive indices of the PIs in the visible region (400−800 nm). The dispersion curves are fitted by the simplified Cauchy's formula (eq 3) and the obtained parameters are listed in Table 3.

Table 3. Wavelength Dispersion of Refractive Indices of the PIs in the Visible Region

	average refractive index						
polyimides	486 nm[a]	589 nm[a]	632.8 nm[a]	656 nm[a]	ν_D[b]	n_∞[c]	D[d] (nm^2)
PI-1	1.7771	1.7400	1.7309	1.7271	14.8	1.6649	26417
PI-2	1.7627	1.7259	1.7162	1.7128	14.6	1.6505	26439
PI-3	1.7902	1.7501	1.7406	1.7368	14.1	1.6700	28291
PI-4	1.7924	1.7516	1.7432	1.7394	14.2	1.6727	28119

[a] Wavelength at which refractive indices were measured. [b] Abbe number defined as eq 2, see Measurements section. [c] Refractive index at infinite wavelength. [d] Coefficient of dispersion. The values of n_∞ and D were obtained from the fitting the wavelength-dependent refractive indices using the simplified Cauchy's formula (eq 3), see Measurements section.

refractive index at infinite wavelength (n_∞) and the coefficients of dispersion (D) are also listed in Table 3.

In accordance with the tradeoff relationship between the refractive indices and the optical transparency as mentioned above, relatively small ν_D values are observed for the PIs exhibiting larger λ_{cutoff} and high n_{633} (PI-3 and PI-4) compared with those with smaller λ_{cutoff} and low n_{633} (PI-1 and PI-2). Further, the former PIs exhibit higher n_∞ and large D than those of the latter. These phenomena are well explained by the theory based on the Drude model or the Lorenz−Lorentz model, which describe the relation between the dispersion (n) and absorption (k) of the complex refractive index (n^*). We have reported that fully aromatic PIs exhibit large coefficients of dispersion (D) of 11930−24190, and the values of D are linearly proportional to n_∞.[41] The small ν_D and the large D values observed for the present PI-1−PI-4 should be related to their long cutoff wavelength (λ_{cutoff}), which causes a steep increase in the refractive index at shorter wavelengths. As listed in Table 3, all the n_{486} values are in the range of 1.7627−1.7924, which are significantly higher than those of PMMA (1.497), PS (1.607), and PC (1.593).

As seen in Table 2, both the flexible sulfonyl and thioether linkages in the molecular chains of the PIs (PI-1 to PI-4) including the ref-PI endow them with very low birefringence (Δn) in the range of 0.0059−0.0068. Note that the PIs containing planar and two-dimensionally polarizable rings of dibenzothiophene (PI-3) and thianthrene (PI-4) also exhibit very small values of Δn. This indicates that the introduction of $-SO_2-$ is effective in prohibiting the in-plane orientation of PI chains. These optically isotropic PI films are desirable for advanced optical fabrications in micro-optics and optical waveguide and circuit applications.

Conclusions

A new *meta*-substituted sulfonyl-bridged dianhydride DPSDA was synthesized and polymerized with four aromatic sulfur-containing diamines to afford a series of high-n PIs. The n_{av} values measured at 632.8 nm range from 1.7162 to 1.7432 depending on the different sulfur contents of the PIs, although they exhibit similar Abbe numbers (ν_D) of 14.1−14.8. The relatively small ν_D values of the PIs, which represent the large wavelength dispersion, lead to very high n_{av} values of 1.7627−1.7924 at 486 nm. The flexible thioether linkages in the PIs endow them with low Δn values in the range of 0.0059−0.0065. The PI films exhibited good optical transmittances exceeding 85% at 450 nm and assumed pale-yellow colors for the thickness of approximately 10 μm due to the existence of the *meta*-substituted bulky electron-withdrawing sulfonyl moieties. Although the T_g values of the proposed PIs are lower than those of the common wholly aromatic PIs, they are still sufficiently high to meet the requirements of optical fabrications. The good combined properties of the present PIs make them good candidates for advanced optical applications.

References and Notes

(1) Ma, H.; Jen, A. K. Y.; Dalton, L. R. *Adv. Mater.* **2002**, *14*, 1339.
(2) Pagliaro, M.; Ciriminna, R. *J. Mater. Chem.* **2005**, *15*, 4981.
(3) Shacklette, L. W. *Opt. Photonics News* **2004**, *15*, 22.
(4) Nakamura, T.; Tsutsumi, N.; Juni, N.; Fujii, H. *J. Appl. Phys.* **2005**, *97*, 054505.
(5) Mikami, A.; Koshiyama, T.; Tsubokawa, T. *Jpn. J. Appl. Phys.* **2005**, *44*, 608.
(6) Ochi, M.; Maeda, Y.; Wakao, K. *Japan J. Net. Polym.* **2006**, *27*, 30 (in Japanese).
(7) Ju, Y. G.; Almuneau, G.; Kim, T. H.; Lee, B. W. *Jpn. J. Appl. Phys.* **2006**, *45*, 2546.
(8) Krogman, K. C.; Druffel, T.; Sunkara, M. K. *Nanotechnology* **2005**, *16*, S338.
(9) Nakai, J.; Aoki, T. U.S. Patent 7,087,945, 2006.
(10) Brandrup, J., Immergut, E. H., Grulke, E. A., Abe, A., Bloch, D. R., Eds. *Polymer Handbook*, 4th ed.; John Wiley & Sons, New York, 2005.
(11) Matsuda, T.; Funae, Y.; Yoshida, M.; Tsuguo, T. *J. Macromol. Sci., Pure Appl. Chem.* **1999**, *A36*, 1271.
(12) Shinichi. K.; Masashi, T.; Hiroaki, M.; Takeshi, F.; Kana, K.; Mitsuaki, Y.; Yasuhiro, S. Jpn. Kokai Tokkyo Koho JP 2005162785, 2005.
(13) Minns, R. A.; Gaudiana, R. A. *J. Macromol. Sci., Pure Appl. Chem.* **1992**, *A29*, 19.
(14) Matsuda, T.; Funae, Y.; Yoshida, M.; Yamamoto, T.; Takaya, T. *J. Appl. Polym Sci.* **2000**, *76*, 45.
(15) Okubo, T.; Kohmoto, S.; Yamamoto, M.; Nakahira, T. *J. Mater. Sci.* **1999**, *34*, 337.
(16) Paquet, C.; Cyr, P. W.; Kumacheva, E.; Manners, I. *Chem. Commun.* **2004**, 234.
(17) Lu, C. L.; Cui, Z. C.; Wang, Y.; Li, Z.; Guan, C.; Yang, B.; Shen, J C. *J. Mater. Chem.* **2003**, *13*, 2189.
(18) Weibel, M.; Caseri, W.; Suter, U. W.; Liess, H.; Wehrli, E. *Polym. Adv. Technol.* **1991**, *2*, 75.
(19) Nussbaumer, R. J.; Caseri, W. R.; Smith, P.; Tervoort, T. *Macromol. Mater. Eng.* **2003**, *288*, 44.
(20) Suwa, M.; Niwa, H.; Tomikawa, M. *J. Photopolym. Sci. Technol.* **2006**, *19*, 275.
(21) Yang, C. P.; Su, Y. Y.; Hsu, M. Y. *Polym. J.* **2006**, *38*, 132.
(22) Terui, Y.; Ando, S. *J. Photopolym. Sci. Technol.* **2005**, *18*, 337.
(23) Yang, C. P.; Chen, Y. P.; Woo, E. M.; Li, S. H. *Polym. J.* **2006**, *38*, 457.
(24) Liu, J. G.; Nakamura, Y.; Shibasaki, Y.; Ando, S.; Ueda, M. *Polym. J.* **2007**, *39*, 543.
(25) Liu, J. G.; Nakamura, Y.; Shibasaki, Y.; Ando, S.; Ueda, M. *J. Polym. Sci. Part A: Polym. Chem.*, **2007**, in press.
(26) Liu, J. G.; Nakamura, Y.; Shibasaki, Y.; Ando, S.; Ueda, M. *Macromol. Chem. Phys.* **2007**, submitted.
(27) Liu, J. G.; Nakamura, Y.; Shibasaki, Y.; Ando, S.; Ueda, M. *Macromolecules* **2007**, *40*, 4614.
(28) Ando, S.; Matsuura, T.; Sasaki, S. *Polym. J.* **1997**, *29*, 69.
(29) Hasegawa, M.; Horie, K. *Prog. Polym. Sci.* **2001**, *26*, 259.
(30) Groh, W.; Zimmermann, A. *Macromolecules* **1991**, *24*, 6660.
(31) Chien, J. C. W.; Cheng, Z. S. *J. Polym. Sci., Part A: Polym. Chem.* **1989**, *27*, 915.

(32) Ando, S.; Fujigaya, T.; Ueda, M. *Jpn. J. Appl. Phys.* **2002**, *41*, L105.
(33) Sugioka, T.; Hay, A. S. *J. Polym. Sci. Part A: Polym. Chem.* **2001**, *39*, 1040.
(34) St. Clair, K.; St. Clair, T. L.; Winfree, W. P. *Proc. ACS Polym. Mater. Sci. Eng.* **1988**, *59*, 28.
(35) Liaw, D. J.; Liaw, B. Y.; Su, K. L. *Polym. Adv. Technol.* **1999**, *10*, 13.
(36) Maier, G. *Prog. Polym. Sci.* **2001**, *26*, 3.
(37) Lee, H. S.; Kim, W. N. *Polymer* **1997**, *38*, 2657.
(38) Nandan, B.; Kandpal, L. D.; Mathur, G. N. *Polymer* **2003**, *44*, 1267.
(39) Noda, Y.; Nakajima, T. *Polym. Prepr. Jpn.* **1986**, *35*, 1245.
(40) Clair, A. K.; Clair T. L. St. U.S. Patent 4,603,061, 1986.
(41) Ando, S.; Watanabe, Y.; Matsuura, T. *Jpn. J. Appl. Phys.* **2002**, *41*, 5254.

MA0713714